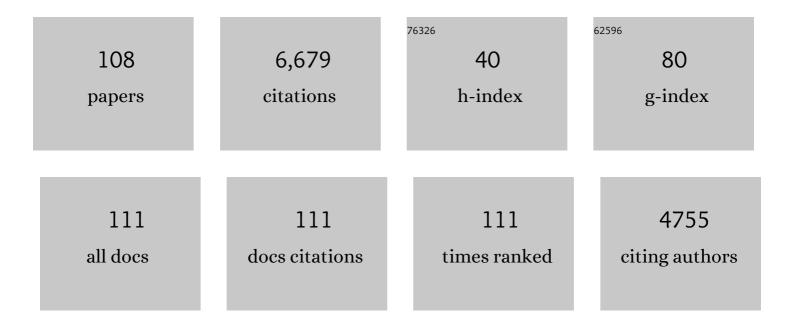
List of Publications by Year in descending order

Source: https://exaly.com/author-pdf/3396295/publications.pdf Version: 2024-02-01



#	Article	IF	CITATIONS
1	Ultrasound Microbubble Contrast Agents: Fundamentals and Application to Gene and Drug Delivery. Annual Review of Biomedical Engineering, 2007, 9, 415-447.	12.3	1,089
2	Microbubble compositions, properties and biomedical applications. Bubble Science, Engineering & Technology, 2009, 1, 3-17.	0.2	444
3	State-of-the-art materials for ultrasound-triggered drug delivery. Advanced Drug Delivery Reviews, 2014, 72, 3-14.	13.7	376
4	Microbubble size isolation by differential centrifugation. Journal of Colloid and Interface Science, 2009, 329, 316-324.	9.4	366
5	Dissolution Behavior of Lipid Monolayer-Coated, Air-Filled Microbubbles:Â Effect of Lipid Hydrophobic Chain Length. Langmuir, 2002, 18, 9225-9233.	3.5	298
6	Ultrasound radiation force enables targeted deposition of model drug carriers loaded on microbubbles. Journal of Controlled Release, 2006, 111, 128-134.	9.9	253
7	Microbubble-Size Dependence of Focused Ultrasound-Induced Blood–Brain Barrier Opening in Mice <i>In Vivo</i> . IEEE Transactions on Biomedical Engineering, 2010, 57, 145-154.	4.2	217
8	Radiation-Force Assisted Targeting Facilitates Ultrasonic Molecular Imaging. Molecular Imaging, 2004, 3, 135-148.	1.4	159
9	Effect of Microbubble Size on Fundamental Mode High Frequency Ultrasound Imaging in Mice. Ultrasound in Medicine and Biology, 2010, 36, 935-948.	1.5	156
10	Microbubble Dissolution in a Multigas Environment. Langmuir, 2010, 26, 6542-6548.	3.5	132
11	DNA and Polylysine Adsorption and Multilayer Construction onto Cationic Lipid-Coated Microbubbles. Langmuir, 2007, 23, 9401-9408.	3.5	127
12	Surface phase behavior and microstructure of lipid/PEG-emulsifier monolayer-coated microbubbles. Colloids and Surfaces B: Biointerfaces, 2004, 35, 209-223.	5.0	121
13	Lateral Phase Separation in Lipid-Coated Microbubbles. Langmuir, 2006, 22, 4291-4297.	3.5	119
14	Microbubble Agents: New Directions. Ultrasound in Medicine and Biology, 2020, 46, 1326-1343.	1.5	118
15	Combined sonodynamic and antimetabolite therapy for the improved treatment of pancreatic cancer using oxygen loaded microbubbles as a delivery vehicle. Biomaterials, 2016, 80, 20-32.	11.4	116
16	Lipid monolayer collapse and microbubble stability. Advances in Colloid and Interface Science, 2012, 183-184, 82-99.	14.7	115
17	State-of-the-art of microbubble-assisted blood-brain barrier disruption. Theranostics, 2018, 8, 4393-4408.	10.0	113
18	Polyplex-microbubble hybrids for ultrasound-guided plasmid DNA delivery to solid tumors. Journal of Controlled Release, 2012, 157, 224-234.	9.9	112

#	Article	IF	CITATIONS
19	A stimulus-responsive contrast agent for ultrasound molecular imaging. Biomaterials, 2008, 29, 597-606.	11.4	103
20	Therapeutic gas delivery via microbubbles and liposomes. Journal of Controlled Release, 2015, 209, 139-149.	9.9	100
21	Oxygen Gas–Filled Microparticles Provide Intravenous Oxygen Delivery. Science Translational Medicine, 2012, 4, 140ra88.	12.4	95
22	The effect of lipid monolayer in-plane rigidity on inÂvivo microbubble circulation persistence. Biomaterials, 2013, 34, 6862-6870.	11.4	93
23	Phospholipid-Stabilized Microbubble Foam for Injectable Oxygen Delivery. Langmuir, 2010, 26, 15726-15729.	3.5	80
24	Microbubble gas volume: A unifying dose parameter in blood-brain barrier opening by focused ultrasound. Theranostics, 2017, 7, 144-152.	10.0	79
25	Ultrasound Radiation Force Modulates Ligand Availability on Targeted Contrast Agents. Molecular Imaging, 2006, 5, 7290.2006.00016.	1.4	74
26	Stability of Monodisperse Phospholipid-Coated Microbubbles Formed by Flow-Focusing at High Production Rates. Langmuir, 2016, 32, 3937-3944.	3.5	74
27	Oxygen Permeability of Fully Condensed Lipid Monolayers. Journal of Physical Chemistry B, 2004, 108, 6009-6016.	2.6	73
28	The role of poly(ethylene glycol) brush architecture in complement activation on targeted microbubble surfaces. Biomaterials, 2011, 32, 6579-6587.	11.4	68
29	Thermal Activation of Superheated Lipid-Coated Perfluorocarbon Drops. Langmuir, 2015, 31, 4627-4634.	3.5	63
30	Methods of Generating Submicrometer Phase-Shift Perfluorocarbon Droplets for Applications in Medical Ultrasonography. IEEE Transactions on Ultrasonics, Ferroelectrics, and Frequency Control, 2017, 64, 252-263.	3.0	62
31	Systemic oxygen delivery by peritoneal perfusion of oxygen microbubbles. Biomaterials, 2014, 35, 2600-2606.	11.4	59
32	Effect of Microstructure on Molecular Oxygen Permeation through Condensed Phospholipid Monolayers. Journal of the American Chemical Society, 2005, 127, 6524-6525.	13.7	56
33	Ligand Conjugation to Bimodal Poly(ethylene glycol) Brush Layers on Microbubbles. Langmuir, 2010, 26, 13183-13194.	3.5	56
34	On the thermodynamics and kinetics of superheated fluorocarbon phase-change agents. Advances in Colloid and Interface Science, 2016, 237, 15-27.	14.7	56
35	Lipid monolayer dilatational mechanics during microbubble gas exchange. Soft Matter, 2012, 8, 4756.	2.7	53
36	Reducing Tumour Hypoxia via Oral Administration of Oxygen Nanobubbles. PLoS ONE, 2016, 11, e0168088.	2.5	52

#	Article	IF	CITATIONS
37	Engineering optically triggered droplets for photoacoustic imaging and therapy. Biomedical Optics Express, 2014, 5, 4417.	2.9	49
38	Enhanced photoacoustic response with plasmonic nanoparticle-templated microbubbles. Soft Matter, 2013, 9, 7743.	2.7	45
39	Lung Surfactant Microbubbles Increase Lipophilic Drug Payload for Ultrasound-Targeted Delivery. Theranostics, 2013, 3, 409-419.	10.0	43
40	Single Microbubble Measurements of Lipid Monolayer Viscoelastic Properties for Small-Amplitude Oscillations. Langmuir, 2016, 32, 9410-9417.	3.5	42
41	Reverse engineering the ultrasound contrast agent. Advances in Colloid and Interface Science, 2018, 262, 39-49.	14.7	41
42	Condensation Phase Diagrams for Lipid-Coated Perfluorobutane Microbubbles. Langmuir, 2014, 30, 6209-6218.	3.5	36
43	Radiation-Force Assisted Targeting Facilitates Ultrasonic Molecular Imaging. Molecular Imaging, 2004, 3, 153535002004041.	1.4	34
44	Effect of Surface Architecture on InÂVivo Ultrasound Contrast Persistence of Targeted Size-Selected Microbubbles. Ultrasound in Medicine and Biology, 2012, 38, 492-503.	1.5	34
45	Click Conjugation of Cloaked Peptide Ligands to Microbubbles. Bioconjugate Chemistry, 2018, 29, 1534-1543.	3.6	31
46	In Vivo Demonstration of Cancer Molecular Imaging with Ultrasound Radiation Force and Buried-Ligand Microbubbles. Molecular Imaging, 2013, 12, 7290.2013.00052.	1.4	27
47	Single-Particle Optical Sizing of Microbubbles. Ultrasound in Medicine and Biology, 2014, 40, 138-147.	1.5	27
48	Application of Elastography for the Noninvasive Assessment of Biomechanics in Engineered Biomaterials and Tissues. Annals of Biomedical Engineering, 2016, 44, 705-724.	2.5	27
49	Fluorocarbon Nanodrops as Acoustic Temperature Probes. Langmuir, 2015, 31, 10656-10663.	3.5	26
50	High Efficiency Molecular Delivery with Sequential Low-Energy Sonoporation Bursts. Theranostics, 2015, 5, 1419-1427.	10.0	25
51	Nanostructural features on stable microbubbles. Soft Matter, 2009, 5, 716-720.	2.7	24
52	Photoacoustic technique to measure temperature effects on microbubble viscoelastic properties. Applied Physics Letters, 2018, 112, 111905.	3.3	23
53	INJECTABLE OXYGEN DELIVERY BASED ON PROTEIN-SHELLED MICROBUBBLES. Nano LIFE, 2010, 01, 215-218.	0.9	22
54	Optically induced resonance of nanoparticle-loaded microbubbles. Optics Letters, 2014, 39, 3732.	3.3	21

#	Article	IF	CITATIONS
55	Phospholipid Oxygen Microbubbles for Image-Guided Therapy. Nanotheranostics, 2020, 4, 83-90.	5.2	20
56	Bubble Inflation Using Phase-Change Perfluorocarbon Nanodroplets as a Strategy for Enhanced Ultrasound Imaging and Therapy. Langmuir, 2020, 36, 2954-2965.	3.5	20
57	Ultrasound-modulated fluorescence based on fluorescent microbubbles. Journal of Biomedical Optics, 2014, 19, 085005.	2.6	19
58	Effect of Hydrostatic Pressure, Boundary Constraints and Viscosity on the Vaporization Threshold of Low-Boiling-Point Phase-Change Contrast Agents. Ultrasound in Medicine and Biology, 2019, 45, 968-979.	1.5	19
59	Lung surfactant microbubbles. Soft Matter, 2009, 5, 4835.	2.7	18
60	Simulation of xâ€rayâ€induced acoustic imaging for absolute dosimetry: Accuracy of image reconstruction methods. Medical Physics, 2020, 47, 1280-1290.	3.0	18
61	Treatment of a Rat Model of LPS-Induced ARDS via Peritoneal Perfusion of Oxygen Microbubbles. Journal of Surgical Research, 2020, 246, 450-456.	1.6	17
62	Perfusion-guided sonopermeation of neuroblastoma: a novel strategy for monitoring and predicting liposomal doxorubicin uptake <i>in vivo</i> . Theranostics, 2020, 10, 8143-8161.	10.0	17
63	Microbubble Size and Dose Effects on Pharmacokinetics. ACS Biomaterials Science and Engineering, 2022, 8, 1686-1695.	5.2	17
64	Intermolecular Forces Model for Lipid Microbubble Shells. Langmuir, 2019, 35, 10042-10051.	3.5	16
65	Vaporizable endoskeletal droplets via tunable interfacial melting transitions. Science Advances, 2020, 6, eaaz7188.	10.3	16
66	Ultrasound-mediated delivery of siESE complexed with microbubbles attenuates HER2+/- cell line proliferation and tumor growth in rodent models of breast cancer. Nanotheranostics, 2019, 3, 212-222.	5.2	15
67	Acoustic nanodrops for biomedical applications. Current Opinion in Colloid and Interface Science, 2020, 50, 101383.	7.4	14
68	The effect of size range on ultrasound-induced translations in microbubble populations. Journal of the Acoustical Society of America, 2020, 147, 3236-3247.	1.1	12
69	In vivo demonstration of cancer molecular imaging with ultrasound radiation force and buried-ligand microbubbles. Molecular Imaging, 2013, 12, 357-63.	1.4	12
70	Acoustically manipulating internal structure of disk-in-sphere endoskeletal droplets. Nature Communications, 2022, 13, 987.	12.8	12
71	Microbubble dispersions of natural lung surfactant. Current Opinion in Colloid and Interface Science, 2014, 19, 480-489.	7.4	11
72	Better contrast with vesicles. Nature Nanotechnology, 2014, 9, 248-249.	31.5	10

#	Article	IF	CITATIONS
73	Hydrostatic Pressurization of Lung Surfactant Microbubbles: Observation of a Strain-Rate Dependent Elasticity. Langmuir, 2017, 33, 13699-13707.	3.5	10
74	Microbubbles and Nanodrops for photoacoustic tomography. Current Opinion in Colloid and Interface Science, 2021, 55, 101464.	7.4	10
75	Plane-Wave Contrast Imaging: A Radiation Force Point of View. IEEE Transactions on Ultrasonics, Ferroelectrics, and Frequency Control, 2018, 65, 2296-2300.	3.0	9
76	Microbubble Radiation Force-Induced Translation in Plane-Wave Versus Focused Transmission Modes. IEEE Transactions on Ultrasonics, Ferroelectrics, and Frequency Control, 2019, 66, 1856-1865.	3.0	9
77	Ultrasound-modulated fluorescence based on donor-acceptor-labeled microbubbles. Journal of Biomedical Optics, 2015, 20, 036012.	2.6	6
78	Pre-clinical assessment of a water-in-fluorocarbon emulsion for the treatment of pulmonary vascular diseases. Drug Delivery, 2019, 26, 147-157.	5.7	6
79	Nanobubbles are Non-Echogenic for Fundamental-Mode Contrast-Enhanced Ultrasound Imaging. Bioconjugate Chemistry, 2022, 33, 1106-1113.	3.6	6
80	Peritoneal Membrane Oxygenation Therapy for Rats With Acute Respiratory Distress Syndrome1. Journal of Medical Devices, Transactions of the ASME, 2016, 10, 020905.	0.7	4
81	The Dependence of the Ultrasound-Induced Blood-Brain Barrier Opening Characteristics on Microbubble Size In Vivo. , 2009, , .		3
82	Changes in microbubble dynamics upon adhesion to a solid surface. Applied Physics Letters, 2020, 116, 123703.	3.3	3
83	Ultrasound Contrast Agents. , 2021, , 639-653.		3
84	Peritoneal Microbubble Oxygenation: An Extrapulmonary Respiration Treatment in Rabbits1. Journal of Medical Devices, Transactions of the ASME, 2014, 8, .	0.7	3
85	Detecting insulitis in type 1 diabetes with ultrasound phase-change contrast agents. Proceedings of the United States of America, 2021, 118, .	7.1	3
86	High-frequency ultrasound imaging of size-isolated microbubbles in mice. , 2009, , .		2
87	Microbubble shell break-up and collapse during gas exchange. , 2010, , .		2
88	Photoacoustic Impulse Response of Lipid-Coated Ultrasound Contrast Agents. IEEE Transactions on Ultrasonics, Ferroelectrics, and Frequency Control, 2021, 68, 2311-2314.	3.0	2
89	Effect of Thermal History and Hydrocarbon Core Size on Perfluorocarbon Endoskeletal Droplet Vaporization. Langmuir, 2022, 38, 2634-2641.	3.5	2
90	An in-vivo evaluation of the effects of anesthesia carrier gases on ultrasound contrast agent		1

circulation., 2009,,.

#	Article	IF	CITATIONS
91	Microbubble lipid shell elasticity: Simulation and measurement. , 2016, , .		1
92	Notice of Removal: Oxygen microbubbles improve tumor control after radiotherapy in a rat fibrosarcoma model. , 2017, , .		1
93	A Study of Radiation Force Effects in Plane-Wave Transmission Mode. , 2018, , .		1
94	Designing Oxygen Microbubbles for Treating Tumor Hypoxia. , 2019, , .		1
95	Contrast-Enhanced Sonography with Biomimetic Lung Surfactant Nanodrops. Langmuir, 2021, 37, 2386-2396.	3.5	1
96	The Treatment of Acute Respiratory Distress Syndrome in Rats With a Peritoneal Dosing System1. Journal of Medical Devices, Transactions of the ASME, 2015, 9, 020929.	0.7	1
97	Enhanced visibility through microbubble-induced photoacoustic fluctuation imaging. JASA Express Letters, 2022, 2, 012001.	1.1	1
98	Comparing tumor response to VEGF blockade therapy using high frequency ultrasound imaging with size-selected microbubble contrast agents. , 2010, , .		0
99	Single microbubble measurements of temperature dependent viscoelastic properties. , 2017, , .		Ο
100	Notice of Removal: Daily intra-tumoral administration of oxygen microbubbles slows tumor growth in the absence of other therapy in a rat subcutaneous fibrosarcoma model. , 2017, , .		0
101	Notice of Removal: Tumor hypoxia modulation dynamics using intra-tumoral, intra-peritoneal and intra-venous oxygen microbubbles administrations — In vivo real-time measurements via spectroscopic absorbance on a rat subcutaneous fibrosarcoma model. , 2017, , .		0
102	Single microbubble measurements of temperature dependent viscoelastic properties. , 2017, , .		0
103	Single Microbubble Measurements for Bound and Unbound Conditions. , 2019, , .		Ο
104	Ultrasound radiation force as a method to characterize the viscosity of microbubble shells. , 2019, , .		0
105	Perfusion-Guided Monitoring of Tumor Response to Sonoporation and Prediction of Liposomal Doxorubicin Uptake Using Microbubble Contrast Agents. , 2019, , .		Ο
106	Single Microbubble Measurements for Bound and Unbound Conditions. , 2019, , .		0
107	Design and Development of a Rat Peritoneal Infusion Device for Oxygen Microbubble Bolus Delivery1. Journal of Medical Devices, Transactions of the ASME, 2016, 10, .	0.7	0
108	Preâ€clinical application of aerosolized waterâ€inâ€fluorocarbon emulsion intrapulmonary drug delivery system for targeting pulmonary vascular diseases. FASEB Journal, 2018, 32, 858.1.	0.5	0